



## Regular article

## Basal-pyramidal dislocation lock in deformed magnesium

B. Li <sup>a,\*</sup>, Q.W. Zhang <sup>a</sup>, S.N. Mathaudhu <sup>b</sup><sup>a</sup> Department of Chemical and Materials Engineering, University of Nevada, Reno, NV 89557, USA<sup>b</sup> Department of Mechanical Engineering, University of California, Riverside, CA 92521, USA

## ARTICLE INFO

## Article history:

Received 7 August 2016

Received in revised form 9 February 2017

Accepted 23 February 2017

Available online xxxx

## Keywords:

Magnesium

Dislocation

Stacking fault

Transmission electron microscopy

## ABSTRACT

Dislocations and stacking faults in unalloyed magnesium processed by equal-channel-angular-extrusion are investigated by transmission electron microscopy. Stacking faults as wide as hundreds of nanometers and complex dislocation configurations are revealed, which creates diffraction contrast that is challenging to interpret. To elucidate the dislocation interaction, atomistic simulations are conducted. The concomitant results show that the leading partial dislocations on the basal and the pyramidal planes interact and form a dislocation lock, creating the diffraction contrast observed in experiments. The dislocation locks may act as obstacles to dislocation glide and contribute to hardening.

© 2017 Acta Materialia Inc. Published by Elsevier Ltd. All rights reserved.

Magnesium and its alloys are being considered for a wide variety of application due to their light weight, high specific strength and availability, however broader application is limited by the low ductility at room temperature [1]. Compared to aluminum (Al) alloys that have face-centered-cubic (fcc) crystal structures, hexagonal-close-packed (hcp) magnesium (Mg) respond to mechanical loading very differently, in part due to complex dislocation structures, and in part due to deformation twinning [2]. In terms of dislocation slip, three different slip planes have been reported in the literature: basal, prismatic and pyramidal systems [3]. The basal dislocation tends to dissociate into two Shockley partials, i.e.  $\frac{1}{3}2\bar{1}\bar{1}0 \rightarrow \frac{1}{3}10\bar{1}0 + SF + \frac{1}{3}1\bar{1}00$ , and a stacking fault (SF) is created between the two partials. Although the basal stacking fault energy (SFE) of Mg is low (25–35 mJ/m<sup>2</sup>), the equilibrium split distance between the Shockley partials is only 1–3 nm [4]. Thus, in conventional transmission electron microscopy (TEM) observations, the basal dislocations usually appear to be non-dissociated [5]. Previous reports also reveal distinct basal SFs which are frequently observed inside  $\{10\bar{1}2\}10\bar{1}\bar{1}$  deformation twins [6–9]. These SFs are generated by incoherent twin boundary migration, and no partial dislocations that bound the SFs are involved [6]. Prismatic dislocations are often observed in deformed polycrystalline Mg in TEM analyses [10,11], but their dissociation is more complex than basal dislocations due to the corrugated nature of the slip plane. Recently, Liao et al. [12] uncovered the unstable dissociation of a prismatic dislocation. Due to the possibly high SFE on

the prismatic plane, the SF was quickly eliminated by the trailing partial. Thus, prismatic dislocations also appear to be full dislocation lines in TEM.

Pyramidal slip in hcp metals has been reported by a number of researchers [13–20]. Two possible pyramidal slip planes were reported:  $\{10\bar{1}1\}$  [13,20–23] and  $\{11\bar{2}2\}$  [14,15,24]. The Burgers vector,  $\frac{1}{3}11\bar{2}\bar{3}$ , i.e. the  $\langle c+a \rangle$ , equals  $a \cdot \sqrt{1+\gamma^2} \approx 0.612$  nm for Mg ( $a$  is the lattice parameter 0.321 nm and  $\gamma$  the  $c/a$  ratio 1.624) is fairly large if compared to other Burgers vectors in pure metals, and this has prompted a number of atomistic simulations to investigate possible dissociations and the resultant SFs [16–23,25,26]. Recently, Wu and Curtin [25] simulated dissociation of a  $\{11\bar{2}2\}11\bar{2}\bar{3}$  pyramidal II dislocation, using a modified embedded atom method (MEAM) [27] potential and long-time atomistic simulations. They revealed basal-dissociated immobile structures that account for the high hardening and low ductility in  $c$ -axis compression.

Due to the complexity, dislocation structures, especially their interactions in hcp Mg have not been thoroughly understood, and the resulting incongruity over slip activity in terms of mechanism and dislocation interactions necessitates further investigation. The purpose of this work is to carefully probe dislocation and SF activities in unalloyed Mg processed by equal-channel-angular-extrusion (ECAE) [28]. Complex diffraction contrast is observed, thus concurrent atomistic simulations are performed to facilitate interpretation of the image contrast. This combination of TEM and atomistic simulations enables unraveling of the complex dislocation interactions in hcp metals.

The starting material was from an as-cast 99.9% purity Norsk Hydro ingot, courtesy of Magnesium Elektron – North America (Madison, IL,

\* Corresponding author.

E-mail address: [binl@unr.edu](mailto:binl@unr.edu) (B. Li).

USA). Its columnar grains had diameters of  $\sim 1.0$  mm and lengths on the order of tens of millimeters. No thermomechanical homogenization pre-processing was done prior to ECAE processing. Rods of 12.5 mm diameter and 50 mm long were processed via route C ( $90^\circ$  channel intersection,  $180^\circ$  rotation about the rod long axis between passes [28]) at  $150^\circ\text{C}$  up to four passes, at a punch speed of 2.54 mm/s without applied backpressure. TEM specimens were prepared by polishing samples to a nominal thickness of  $130\ \mu\text{m}$  using a series of sand paper down to grit number 800. Three millimeter discs were then mechanically punched from the sample. Specimens were then polished using a Tenupol-3 electropolisher with an electrolyte (0.5% perchloric acid + 20% nitric acid + ethanol). The specimens were then cleaned by ion-milling for about 0.5 h with liquid nitrogen cooling and very gentle milling conditions (low incidental angle and low voltage). TEM observations were carried out on a Philips 420 microscope with a double-tilt specimen stage, and an accelerating voltage of 120 kV. After four passes of ECAE, the grain structure was significantly refined with an average grain size of  $3.0\ \mu\text{m}$ . The overall microstructure is inhomogeneous with regions of fine grains from dynamic recrystallization and other regions of relatively large grains which are heavily deformed but not recrystallized.

To further elucidate our experimental observations, atomistic simulations were performed which predictively model the interaction between the basal slip and the pyramidal dislocations and the resultant SFs. The MD simulations were carried out with a box size of  $40 \times 40 \times 40$  nm containing about 2.8 million Mg atoms. Embedded atom method (EAM) potentials [29,30] for Mg-Al alloy systems were used in our simulations. These potentials were well developed by Liu et al. [31] and have been used in numerous atomistic simulations of Mg and Mg alloys [20,32,33]. The lattice was oriented such that a shear strain was applied parallel to the  $\{10\bar{1}2\}$  plane and along the  $10\bar{1}\bar{1}$  direction. The strain rate was about  $10^8/\text{s}$ . No periodic boundary condition was applied such that heterogeneous nucleation of dislocations at free surfaces was enabled. Constant temperature at 10 K was maintained throughout the simulation. No dislocations were pre-constructed. During shear deformation, slip systems on the basal, prismatic and pyramidal planes all can be activated, and interactions between these slip systems can be investigated.

Fig. 1a shows an array of stacking faults (SFs) in a specimen after two passes at  $150^\circ\text{C}$ . The SFs are quite well-defined with visible bright/dark fringes in the bright-field micrograph. The fringes are similar to what are typically observed in fcc crystals [34], but the dark/bright contrast disrupts at some locations and no longer becomes complementary. This change in the contrast indicates that overlapping SFs are present [34]. At the ends of the SFs, dark contrast typical of dislocations can be observed, as indicated by the block arrow. Fig. 1b displays a weak-beam-dark-field (WBDF) image which confirms the presence of the overlapping SFs. As indicated by the block arrows, two SFs overlap with each other.

The contrast of the SFs dramatically changes when the specimen is tilted to the  $2\bar{1}\bar{1}0$  zone axis. During tilting, the well-defined fringes gradually lose the bright/dark characteristic features, as shown in Fig. 2a. When the zone axis  $2\bar{1}\bar{1}0$  is reached, the fringes of SFs disappear and the contrast becomes straight lines decorated with dark contrast. Close examination reveals that each of these lines is made up of a number of individual segments (indicated by the red arrows) that are well aligned parallel to the trace of the basal plane. Meanwhile, dislocation lines that are parallel to the trace of the basal plane can be observed, as indicated by the black arrows. Because the electron beam is parallel to the basal plane of the specimen, these dislocation lines can be identified as basal dislocations. To identify the Burgers vector of the defects Figs. 1a, b and 2a, we performed WBDF imaging and the result is shown in Fig. 2b. With  $g = 0002$ , the features show a strong  $\langle c \rangle$  component.

The presence of the dislocation contrast at the ends of the SFs (Fig. 1a) indicates that the formation mechanism of these SFs differs from the non-equilibrium basal SFs observed inside deformation twins

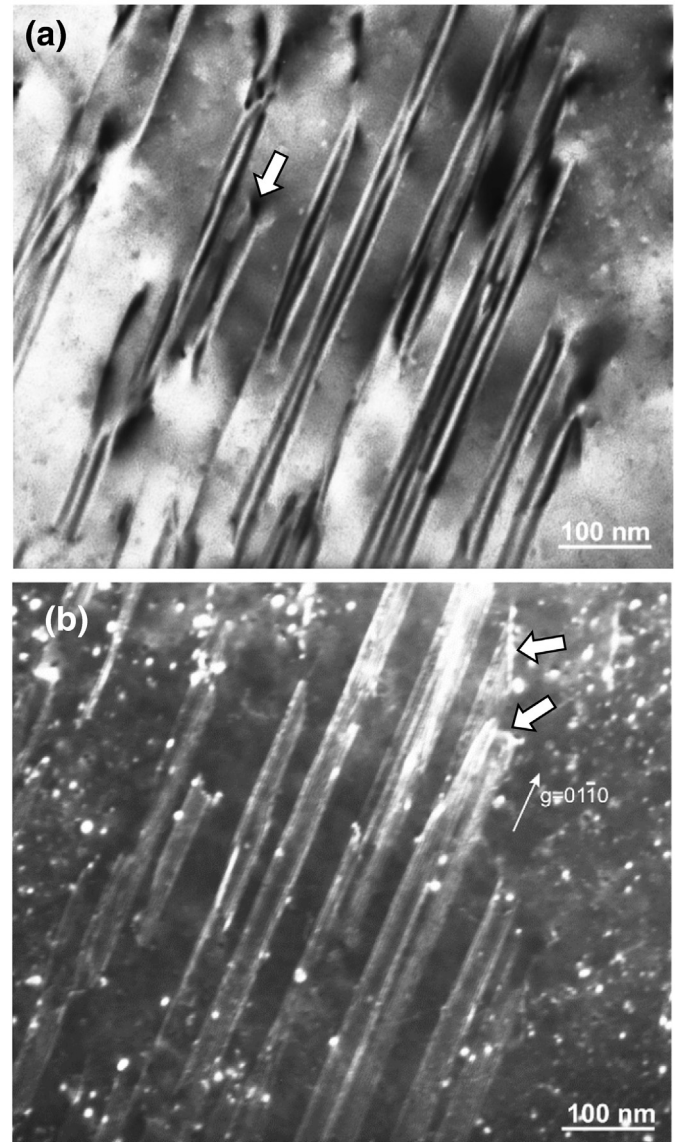


Fig. 1. (a) Bright/dark fringes of SFs with a high density were observed in a specimen after two passes via route C. The widths of the SFs are on the order of hundreds of nanometers. Locations where the dark/bright contrast disrupts indicate that SFs are overlapping. The dark contrast at the end of the SF (denoted by the block arrow) indicates the presence of a partial dislocation. (b) Weak-beam-dark-field (WBDF) image clearly shows the overlapping SFs (indicated by the block arrows).

[6–9]. Zhang et al. recently showed that SFs that may cross a whole twin are not generated by Shockley partial dislocations, but rather, by incoherent twin boundary migration [6]. On the other hand, the width of the SFs in Fig. 1 are as wide as hundreds of nanometers, several orders of magnitude wider than that of the equilibrium width of basal SFs generated by the split of a basal dislocation (1–3 nm [35]). These facts suggest that the SFs in Fig. 1 are likely non-basal SFs. We can also exclude the possibility that these SFs are generated by prismatic slip because the split distance between the partial dislocations of prismatic slip is very small ( $< 1.0$  nm) [12]. Intriguing questions arise from these TEM observations: if the SFs are indeed non-basal, how the contrast of the straight lines (Fig. 2b) parallel to the trace of the basal plane is produced? If the straight lines are associated with the basal slip, why they present a strong  $\langle c \rangle$  component in the Burgers vector analysis?

In the following, we show atomistic simulation results that reveal basal and pyramidal dislocation reaction. Fig. 3a shows a 2-D snapshot of the dislocations that were activated during shear deformation. In

Download English Version:

<https://daneshyari.com/en/article/5443530>

Download Persian Version:

<https://daneshyari.com/article/5443530>

[Daneshyari.com](https://daneshyari.com)